A Novel Approach for Analytical Modeling of Line Commutated Converter based HVDC Systems for Electromagnetic Transient Analysis

Leonhard Probst[1], *Student Member, IEEE*, Christoph Hahn[2], *Member, IEEE*, and Matthias Luther[3], *Member, IEEE*
Chair of Electrical Energy Systems, University of Erlangen-Nuremberg
Erlangen, Germany
[1]leonhard.probst@fau.de, [2]christoph.hahn@fau.de, [3]matthias.luther@fau.de

***Abstract*—A novel approach is used to derive a completely analytical model of a six pulse line commutated converter based HVDC system. The system is split into two subsystems and is then solved individually. Therefore each period of a subsystem is divided into six intervals. Hence it is only necessary to solve one period analytically for the state of commutation as well as for the state of two-valve conduction. All other solutions are then deduced from the original solution with a simple rotation. Afterwards the subsystems are connected and the dependencies of each other are taken into consideration. The space vector transformation is used to split the system into independent subsystems (two for the state of commutation and one for the state of two-valve conduction), which allows to obtain a closed form solution. Accuracy of the model is approved by comparison with electromagnetic transient models.**

***Index Terms*—Analytical models, HVDC transmission, Power system modeling, Space vector transformation.**

I. Introduction

A reliable, economic and environmental friendly supply of electric power is essential for every developed country. The reduction of CO_2 emissions as well as the renunciation of nuclear power are the current challenges for the German transmission system. More and more renewable energy sources like onshore and offshore wind farms, solar power and biomass power stations have to be integrated in the power system. Obviously the load centers are situated in many cases far away from the generation sites. The high voltage DC (HVDC) transmission is the ideal technology to deal with this task [1].

In the last decades, many advancements in power electronics have been achieved. This is the driving force behind the great importance of HVDC systems in power systems nowadays. HVDC allows power transport over long distances with low losses. Developing countries like India [2] and China [3] with a fast growing power capacity are installing more and more HVDC systems for long distance bulk power transmission. But also in relatively small countries like Germany, HVDC systems are in planning to transport renewable generated power, e.g. from offshore wind farms, from the north to the industrial consumers in the south [4].

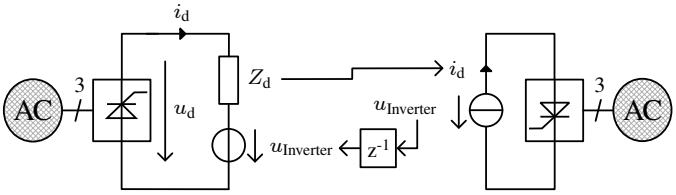

Fig. 1: HVDC splitting with dependent generators

Recently a lot of development has been achieved in the area of voltage sourced converter (VSC) based HVDC systems [1]. But nevertheless line commutated converter (LCC) based HVDC systems are still the best choice for bulk power transmission due to their high current and voltage capability [3]. To be able to design the various subsystems of an HVDC system efficiently and accurately, proper models of these switching systems are needed. Such models are furthermore required to study the considerable interaction with the AC grid in power system analysis. In addition a deeper understanding about functioning of an HVDC system can be obtained by recognizing the fundamental correlations in the models for these power electronic based systems.

Analytical models have been proposed in literature for LCC based HVDC systems [5]. However the approach in this paper is more general and more systematic. The model is not only valid for the steady state, but it can also be used for transient analysis. Furthermore symmetries in the three phase, six pulse converter are used to minimize redundancies in the solutions. The symmetrical three phase system can be simplified with the use of the space vector transformation [6] and the 60° symmetry of the converter can be used to refer the solutions for each state to a fundamental prototype. The rectifier and the inverter are solved independently and the solutions are combined afterwards as depicted in Fig. 1. To verify the approach, the analytical model has been implemented in MATLAB® and will be compared with already existing numerical models in SIMULINK®.

II. Analytical Modelling

In order to provide the analytical solution of the HVDC system, the equations of state have to be derived. To be able to describe the network analytically, some simplifications have to be introduced. The thyristors are regarded ideal and lossless, which means that they are free running or shorted. If a thyristor is free running, its admittance is equal to zero. If it is shorted, the impedance is equal to zero. Furthermore the source is considered ideal and stiff and all impedances are regarded ohmic and inductive.

In the next sections, a rectifier and an inverter are described analytically and afterwards both are combined to an HVDC system. The HVDC system shall be described with space vector and zero-sequence component and be solved independently in the real and imaginary part network.

In order to be able to describe the equal phase displacement of a three phase system, the spin operator $\underline{a}$ as shown in (1) is defined.

$$\underline{a} = e^{j120^\circ} \tag{1}$$

The space vector $\underline{v}$ and the corresponding zero-sequence component v_0 are defined in (2), where g_n are the original values of the three phase system.

$$\begin{pmatrix} 2v_0 \\ \underline{v} \\ \underline{v}^* \end{pmatrix} = \frac{2}{3} \begin{pmatrix} 1 & 1 & 1 \\ 1 & \underline{a} & \underline{a}^2 \\ 1 & \underline{a}^2 & \underline{a} \end{pmatrix} \begin{pmatrix} g_1 \\ g_2 \\ g_3 \end{pmatrix} \tag{2}$$

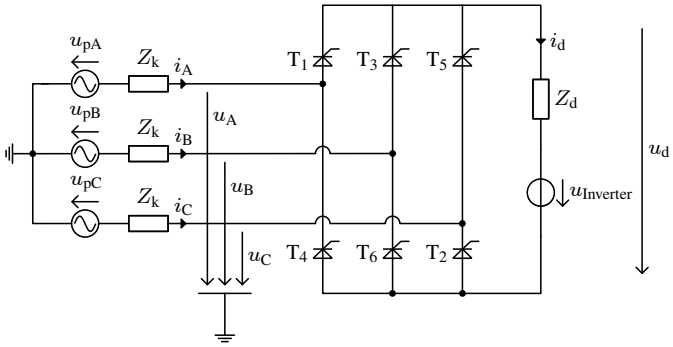

(a) Rectifier

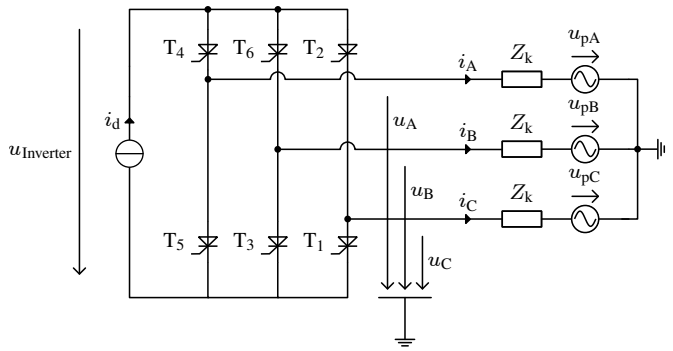

(b) Inverter

Fig. 2: Equivalent circuits of a split HVDC system

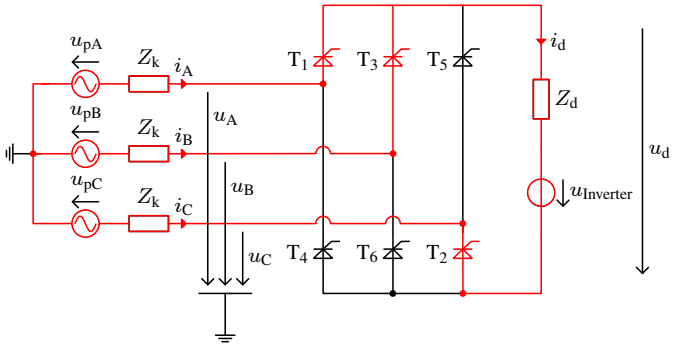

Fig. 3: Rectifier in COM123

The rectifier and the inverter are connected to the grid through a transformer, which is represented by a voltage source in series with a short circuit impedance (Thévenin equivalent). The regarded source is a symmetrical, three phase synchronous voltage as defined in (3). The grid short circuit impedance is represented by Z_k and the DC side of the HVDC system is modeled with a series impedance Z_d as depicted in Fig. 2.

$$\begin{aligned} \underline{u}_p &= \frac{2}{3}\left(u_{pA} + \underline{a}u_{pB} + \underline{a}^2 u_{pC}\right) = \\ &= \frac{2}{3}\left(\hat{U}_p \cos(\omega t) + \hat{U}_p e^{j120^\circ} \cos(\omega t - 120^\circ) + \right. \\ &\left. + \hat{U}_p e^{j240^\circ} \cos(\omega t - 240^\circ)\right) = \hat{U}_p e^{j\omega t} \end{aligned} \tag{3}$$

A. Rectifier

The investigated circuit of the rectifier is shown in Fig. 2a. During the operation of the rectifier, two states need to be taken into consideration. In the state of commutation (COM), the current is redirected from one valve to another. Therefore three valves are conducting current at the same time. Opposite to this, in the state of two-valve conduction (TVC) only two valves are conducting current simultaneously. In normal mode of operation, the state of COM is always started externally with a firing pulse and the state of TVC starts once the current has completely commutated from one valve to another.

1) State of commutation: To be able to describe the state of COM easier, a commutation current i_k is used as defined in [6, p. 5 et seq.]. i_k is half of the difference between the current in the valve with decreasing current (down commutation) and the valve with increasing current (up commutation). This relation can be written mathematically as shown in (4). The direction of the positive current is given through the sources of the three phase system as depicted in Fig. 2a.

$$i_k = \frac{1}{2}\left(i_{ValveDown} - i_{ValveUp}\right) \tag{4}$$

The derivation of the equations of state shall be demonstrated by a specific example. The state of COM123 for the rectifier will be discussed as depicted in Fig. 3. In this state the current of the rectifier is commutating from valve 1 to valve 3. The equations for all other states for both the rectifier and the inverter can be obtained similarly.

The conditions perturbing the symmetrical operation for the currents are defined as follows:

$$\begin{aligned} i_\mathrm{d} &= i_\mathrm{Valve1} + i_\mathrm{Valve3} = i_\mathrm{A} + i_\mathrm{B} \ , \\ 2i_\mathrm{k} &= i_\mathrm{Valve1} - i_\mathrm{Valve3} = i_\mathrm{A} - i_\mathrm{B} \ , \\ i_\mathrm{C} &= i_\mathrm{Valve2} = -i_\mathrm{d} \ . \end{aligned} \tag{5}$$

i_A and i_B can be explicitly written as:

$$\begin{aligned} i_\mathrm{A} &= \frac{1}{2}\left(i_\mathrm{d} + 2i_\mathrm{k}\right) = \frac{i_\mathrm{d}}{2} + i_\mathrm{k} \ , \\ i_\mathrm{B} &= \frac{1}{2}\left(i_\mathrm{d} - 2i_\mathrm{k}\right) = \frac{i_\mathrm{d}}{2} - i_\mathrm{k} \ . \end{aligned} \tag{6}$$

The space vector can be calculated with the currents of all three phases:

$$\begin{aligned} \underline{i}_{123} &= \frac{2}{3}\left(i_\mathrm{A} + \underline{\mathrm{a}} i_\mathrm{B} + \underline{\mathrm{a}}^2 i_\mathrm{C}\right) = \\ &= \frac{2}{3}\left(\frac{i_\mathrm{d}}{2} + i_\mathrm{k} + \underline{\mathrm{a}}\left(\frac{i_\mathrm{d}}{2} - i_\mathrm{k}\right) + \underline{\mathrm{a}}^2\left(-i_\mathrm{d}\right)\right) = \\ &= -\underline{\mathrm{a}}^2 i_\mathrm{d} + \frac{2}{3}\left(1 - \underline{\mathrm{a}}\right) i_\mathrm{k} = \mathrm{e}^{\mathrm{j}60^\circ} i_\mathrm{d} + \frac{2}{\sqrt{3}}\mathrm{e}^{-\mathrm{j}30^\circ} i_\mathrm{k} \ . \end{aligned} \tag{7}$$

The two parts of the space vector $\underline{i}$ are orthogonal to each other ($\hat{=}$ phase displacement is $90°$). Thus they can be separated into two independent networks with a rotation by $-60°$:

$$\begin{aligned} &\underline{i}_{123}\mathrm{e}^{-\mathrm{j}60^\circ} = \mathrm{e}^{\mathrm{j}0^\circ} i_\mathrm{d} + \frac{2}{\sqrt{3}}\mathrm{e}^{-\mathrm{j}90^\circ} i_\mathrm{k} = i_\mathrm{d} - \mathrm{j}\frac{2}{\sqrt{3}} i_\mathrm{k} \ , \\ &\mathrm{Re}\left\{\underline{i}_{123}\mathrm{e}^{-\mathrm{j}60^\circ}\right\} = i_\mathrm{d} \ , \\ &\mathrm{Im}\left\{\underline{i}_{123}\mathrm{e}^{-\mathrm{j}60^\circ}\right\} = -\frac{2}{\sqrt{3}} i_\mathrm{k} \ . \end{aligned} \tag{8}$$

The conditions perturbing the symmetrical operation for the voltages are defined as follows:

$$\begin{aligned} u_\mathrm{A} &= u_\mathrm{B} \ , \\ u_\mathrm{C} &= -u_\mathrm{Inverter} - Z_\mathrm{d} i_\mathrm{d} + u_\mathrm{B} \ . \end{aligned} \tag{9}$$

The space vector of the voltage can be calculated with the voltages of all three phases:

$$\begin{aligned} \underline{u}_{123} &= \frac{2}{3}\left(u_\mathrm{A} + \underline{\mathrm{a}} u_\mathrm{B} + \underline{\mathrm{a}}^2 u_\mathrm{C}\right) = \frac{2}{3}\left(u_\mathrm{A} + \underline{\mathrm{a}} u_\mathrm{A} + \right. \\ &\left. + \underline{\mathrm{a}}^2\left(-u_\mathrm{Inverter} - Z_\mathrm{d} i_\mathrm{d} + u_\mathrm{A}\right)\right) = -\frac{2}{3}\underline{\mathrm{a}}^2 \cdot \\ &\cdot \left(u_\mathrm{Inverter} + Z_\mathrm{d} i_\mathrm{d}\right) = -\frac{2}{3}\mathrm{e}^{\mathrm{j}240^\circ}\left(u_\mathrm{Inverter} + Z_\mathrm{d} i_\mathrm{d}\right) \ . \end{aligned} \tag{10}$$

As the space vector of the currents has been rotated, the space vector of the voltages must be rotated, too:

$$\begin{aligned} \underline{u}_{123}\mathrm{e}^{-\mathrm{j}60^\circ} &= -\frac{2}{3}\mathrm{e}^{\mathrm{j}180^\circ}\left(u_\mathrm{Inverter} + Z_\mathrm{d} i_\mathrm{d}\right) = \\ &= \frac{2}{3}\left(u_\mathrm{Inverter} + Z_\mathrm{d} i_\mathrm{d}\right) \ . \end{aligned} \tag{11}$$

The equivalent circuit diagrams for the state of COM are depicted in Fig. 4 for the general case. The individual commutation states differ only in a phase rotation indicated by the rotation index n. Both networks are linear differential equations of first order and can be solved analytically. The closed form solutions for the DC current i_d and the the commutation current i_k are listed in (13). In order to simplify the solutions, some substitutions are used:

$$\begin{aligned} R &\coloneqq R_\mathrm{k} + \frac{2}{3} R_\mathrm{d} \ , \\ X &\coloneqq X_\mathrm{k} + \frac{2}{3} X_\mathrm{d} \ , \\ \phi &\coloneqq \varphi - 60^\circ n \ . \end{aligned} \tag{12}$$

For the purpose of calculating the phase currents out of the state variables, the space vector is composed with the right rotation angle according to the current commutation state. The phase currents can then be obtained with the use of the inverse space vector transformation.

$$\begin{aligned} i_\mathrm{d} &= \hat{U}_\mathrm{p} \frac{\cos\left(\omega t + \phi - \mathrm{atan}\left(\frac{X}{R}\right)\right)}{\sqrt{R^2 + X^2}} - \hat{U}_\mathrm{p}\mathrm{e}^{-\frac{R}{X}\omega(t - \mathrm{t}_0)} \\ &- \frac{\cos\left(\omega \mathrm{t}_0 + \phi - \mathrm{atan}\left(\frac{X}{R}\right)\right)}{\sqrt{R^2 + X^2}} - \frac{2}{3X}\mathrm{e}^{-\frac{R}{X}\omega t} \cdot \\ &\cdot \int_{\omega \mathrm{t}_0}^{\omega t} u_\mathrm{Inverter}\mathrm{e}^{\frac{R}{X}\omega\tau}\,\mathrm{d}(\omega\tau) + i_\mathrm{d}(\mathrm{t}_0)\ \mathrm{e}^{-\frac{R}{X}\omega(t - \mathrm{t}_0)} \ , \\ i_\mathrm{k} &= -\frac{\sqrt{3}}{2}\hat{U}_\mathrm{p} \frac{\sin\left(\omega t + \phi - \mathrm{atan}\left(\frac{X_\mathrm{k}}{R_\mathrm{k}}\right)\right)}{\sqrt{R_\mathrm{k}^2 + X_\mathrm{k}^2}} + \frac{\sqrt{3}}{2}\hat{U}_\mathrm{p} \cdot \\ &\cdot \frac{\sin\left(\omega \mathrm{t}_0 + \phi - \mathrm{atan}\left(\frac{X_\mathrm{k}}{R_\mathrm{k}}\right)\right)}{\sqrt{R_\mathrm{k}^2 + X_\mathrm{k}^2}} \mathrm{e}^{-\frac{R_\mathrm{k}}{X_\mathrm{k}}\omega(t - \mathrm{t}_0)} + \\ &+ i_\mathrm{k}(\mathrm{t}_0)\ \mathrm{e}^{-\frac{R_\mathrm{k}}{X_\mathrm{k}}\omega(t - \mathrm{t}_0)} \ , \\ \underline{i} &= \left(i_\mathrm{d} - \mathrm{j}\frac{2}{\sqrt{3}} i_\mathrm{k}\right)\mathrm{e}^{\mathrm{j}60^\circ n} \end{aligned} \tag{13}$$

2) State of two-valve conduction: For the state of TVC, there is only one equivalent circuit (Fig. 5) as the commutation current is zero per definition. The solution for the DC current i_d is shown in (15). The space vector for this state only depends on the DC current and on the rotation index n according to the regarded TVC state. As for the state of COM, again some substitutions are used in order to be able to write the solutions in a compact manner:

$$\begin{aligned} R &\coloneqq R_\mathrm{k} + \frac{1}{2} R_\mathrm{d} \ , \\ X &\coloneqq X_\mathrm{k} + \frac{1}{2} X_\mathrm{d} \ , \\ \phi &\coloneqq \varphi - 60^\circ n \ . \end{aligned} \tag{14}$$

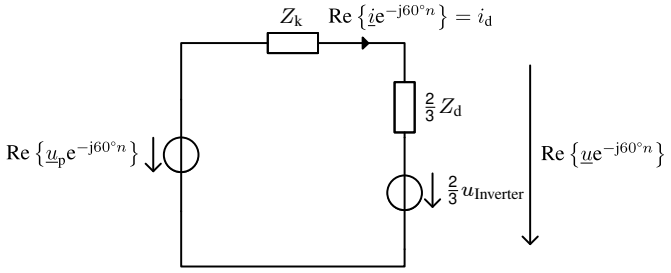

(a) Real part network

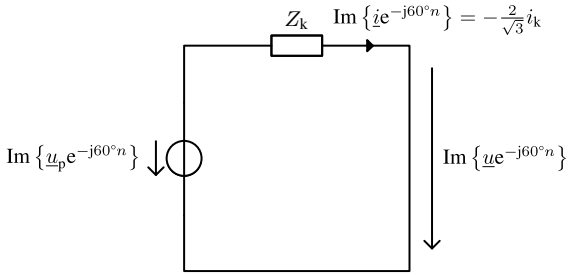

(b) Imaginary part network

Fig. 4: Space vector equivalent circuits of a rectifier in state of commutation

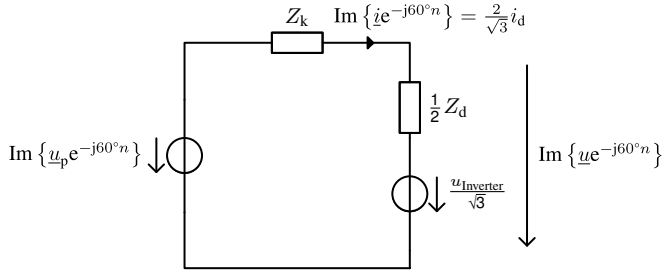

Fig. 5: Space vector equivalent circuit of a rectifier in state of two-valve conduction

$$
\begin{aligned}
i_\mathrm{d} = {} & \frac{\sqrt{3}}{2}\hat{U}_\mathrm{p}\frac{\sin\left(\omega t + \phi - \operatorname{atan}\left(\frac{X}{R}\right)\right)}{\sqrt{R^2+X^2}} - \frac{\sqrt{3}}{2}\hat{U}_\mathrm{p}\cdot \\
& \cdot \mathrm{e}^{-\frac{R}{X}\omega(t-\mathrm{t}_0)}\frac{\sin\left(\omega \mathrm{t}_0 + \phi - \operatorname{atan}\left(\frac{X}{R}\right)\right)}{\sqrt{R^2+X^2}} - \\
& - \frac{1}{2X}\mathrm{e}^{-\frac{R}{X}\omega t}\int_{\omega \mathrm{t}_0}^{\omega t} u_\mathrm{Inverter}\mathrm{e}^{\frac{R}{X}\omega\tau}\,\mathrm{d}(\omega\tau) + \\
& + i_\mathrm{d}(\mathrm{t}_0)\ \mathrm{e}^{-\frac{R}{X}\omega(t-\mathrm{t}_0)}\ , \\
\underline{i} = {} & \mathrm{j}\frac{2}{\sqrt{3}}i_\mathrm{d}\mathrm{e}^{\mathrm{j}60°n}
\end{aligned}
\tag{15}
$$

B. Inverter

The inverter is regarded as depicted in Fig. 2b. The analytical characterization is similar as for the rectifier, but as a current source instead of a voltage source is used for the model, the system becomes easier to analyze. The DC current i_d is constant for both the COM and the TVC states. Therefore only one analytical solution for the commutation current i_k in the state of COM has to be derived.

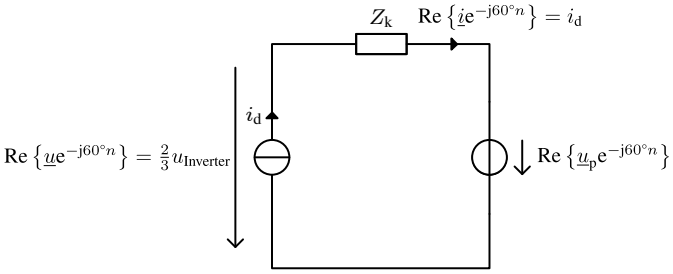

(a) Real part network

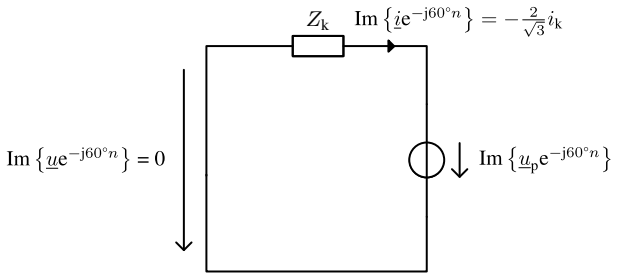

(b) Imaginary part network

Fig. 6: Space vector equivalent circuits of an inverter in state of commutation

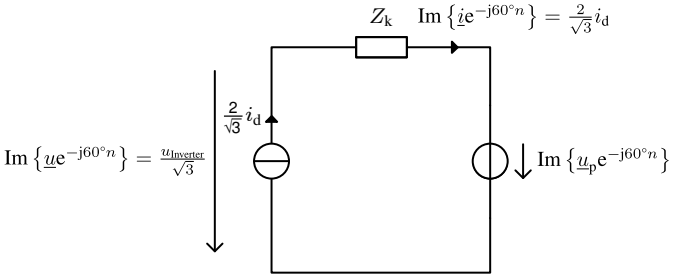

Fig. 7: Space vector equivalent circuit of an inverter in state of two-valve conduction

1) State of commutation: The current i_k flows in the imaginary part network for the state of COM as depicted in Fig. 7. The network is again a linear differential equation of first order and can be solved analytically. The solution is listed in (16) together with the composition rule for the space vector. The substitution for the angle ϕ of (12) is again used to simplify the solution.

$$
\begin{aligned}
i_\mathrm{k} = {} & \frac{\sqrt{3}}{2}\hat{U}_\mathrm{p}\frac{\sin\left(\omega t + \phi - \operatorname{atan}\left(\frac{X_\mathrm{k}}{R_\mathrm{k}}\right)\right)}{\sqrt{R_\mathrm{k}^2+X_\mathrm{k}^2}} - \frac{\sqrt{3}}{2}\hat{U}_\mathrm{p}\cdot \\
& \cdot \frac{\sin\left(\omega \mathrm{t}_0 + \phi - \operatorname{atan}\left(\frac{X_\mathrm{k}}{R_\mathrm{k}}\right)\right)}{\sqrt{R_\mathrm{k}^2+X_\mathrm{k}^2}}\mathrm{e}^{-\frac{R_\mathrm{k}}{X_\mathrm{k}}\omega(t-\mathrm{t}_0)} + \\
& + i_\mathrm{k}(\mathrm{t}_0)\ \mathrm{e}^{-\frac{R_\mathrm{k}}{X_\mathrm{k}}\omega(t-\mathrm{t}_0)}\ , \\
\underline{i} = {} & \left(i_\mathrm{d} - \mathrm{j}\frac{2}{\sqrt{3}}i_\mathrm{k}\right)\mathrm{e}^{\mathrm{j}60°n}
\end{aligned}
\tag{16}
$$

2) State of two-valve conduction: The solution for the state of TVC is simple as the network consists only of one path with

TABLE I: Mapping table

n	0	1	2	3	4	5
Rect. COM	COM612	COM123	COM234	COM345	COM456	COM561
Rect. TVC	TVC23	TVC34	TVC45	TVC56	TVC61	TVC12
Inv. COM	COM345	COM456	COM561	COM612	COM123	COM234
Inv. TVC	TVC56	TVC61	TVC12	TVC23	TVC34	TVC45

a current source in it. Hence the current is equal throughout the circuit and the according space vector can be built like shown in (17).

$$\underline{i} = \mathrm{j}\frac{2}{\sqrt{3}} i_\mathrm{d} \mathrm{e}^{\mathrm{j}60^\circ n} \tag{17}$$

Now the solutions for all possible states of an HVDC system during normal mode of operation have been derived. In order to verify the approach, a time domain simulation shall be implemented. Therefore the transitions between the different states have to be analyzed in advance.

III. Implementation

The state transition diagram is shown in Fig. 8. In normal mode of operation, the transition will always occur either from one state of COM to the next state of COM or to an intermediate state of TVC. One such transition is shown in orange as an example in the transition diagram. At first the converter is in the state of TVC23, which means that valve 2 and valve 3 are conducting. Now the commutation to valve 4 is initiated by a firing impulse. Therefore the converter enters the state of COM234. In order to obtain the right solutions for that state, a rotation by -120° is needed. After the current has fully commutated, the converter shifts to the state of TVC34. According to the transition diagram, a rotation by +60° is needed. To sum up the example, one can say that a rotation by -120° has to be performed to shift from a state of TVC to the next state of COM, and a rotation by +60° is needed to shift from there to the next state of TVC. The example is also illustrated in (18).

$$\text{TVC23} \xrightarrow{n+=2} \text{COM234} \xrightarrow{n-=1} \text{TVC34} \tag{18}$$

As the inverter can be seen as a rectifier flipped by 180° along the horizontal axis, one can easily expect that also the solutions for the inverter are phase shifted by 180°. So for example the phase angle for the state of COM123 is -60° for the rectifier and +120° for the inverter. All states for both the rectifier and the inverter with their given rotation index n are listed in TABLE I.

The flowchart of the program is depicted in Fig. 9. The program starts with the definition of various states of the HVDC system and of the simulation variables itself. Afterwards the main loop is entered and is iterated until the simulation time fulfills the stop condition. At first the solutions for the rectifier are calculated dependent on its state (TVC or COM). Therefore the solution of the inverter of the previous iteration step has to be taken into consideration because both converters

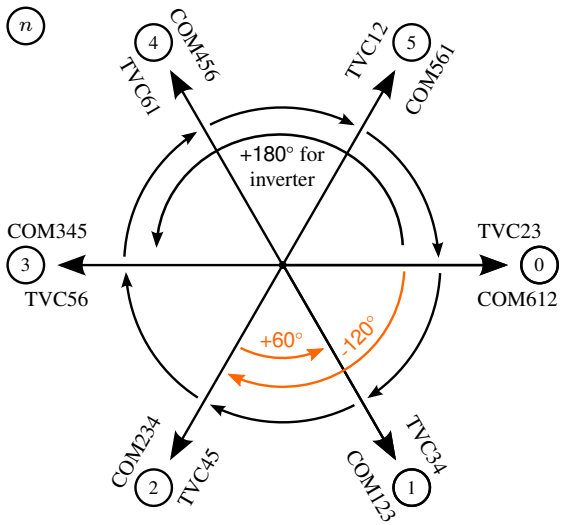

Fig. 8: State transition diagram

TABLE II: Parameter set of regarded HVDC system

f	50 Hz
$\hat{U}_\mathrm{p}$	163.3 kV
$\alpha_\mathrm{Rectifier}$	5°
α_Inverter	160°
R_k	0.35 Ω
L_k	11.1 mH
R_d	0.1 Ω
L_d	85 mH

are connected as shown in Fig. 1. After that the inverter is also calculated on the basis of its state (TVC or COM). Here the solution of the rectifier of the current iteration step is needed, too, due to the interconnection of both converters. As all states have been calculated, the transition is checked both for the rectifier and the inverter. It is determined if a new COM or TVC state starts either in the rectifier or in the inverter. Once all calculations are done, the program puts the simulation data in appropriate form and the output is generated.

IV. Results

The results of the analytical model in MATLAB® and the electromagnetic transient (EMT) model in Simulink® using the SimPowerSystems toolbox shall be compared. A common parameter set for a back-to-back HVDC system has been used for all following simulations. The most important values are listed in TABLE II. This realistic set has been taken over from [7, p. 3], nevertheless it has been slightly adopted to get more informative results.

The observed simulation period is 200 ms. Each simulation starts firing the valves at 20 ms. The currents of the rectifier are depicted in Fig. 10. These currents are shown in more detail for the start-up period in Fig. 11 for the rectifier and in Fig. 12 for the inverter. The output voltage of the rectifier for the analytical model and the EMT model is compared in Fig. 13 for the start-up period.

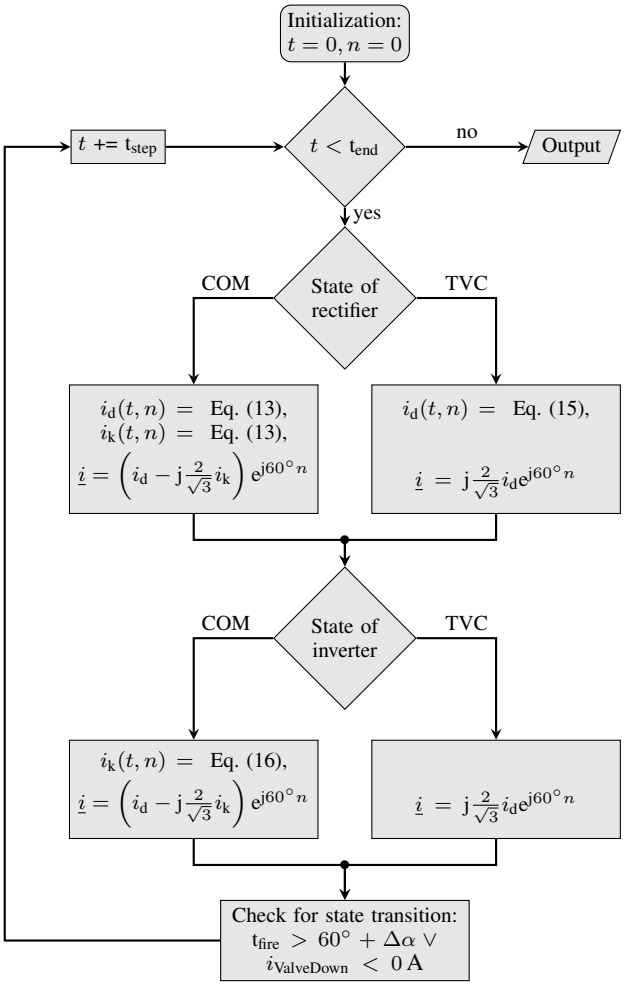

Fig. 9: Flow chart of time domain simulation

In order to analyze the difference of both simulations more in detail, the deviation from each other for the DC current i_d is depicted in Fig. 14. The difference is calculated according to (19). It shows that the maximum deviation is way less than one per mille, which should be accurate enough for most cases of application.

$$\delta = \frac{i_d - i_{d,\,EMT}}{\max(i_{d,\,EMT})} \tag{19}$$

V. Conclusion

With this model detailed analyses of LCC based HVDC systems in power system studies are now possible. As closed form solutions have been found for the state of COM as well as for the state of TVC, a highly accurate simulation in the time domain with very less computational effort can be carried out. Not the minimum time step like for numerical simulations is important for the accuracy, but instead the number of switching points (transition of states) which have to be detected. Furthermore basic understanding of the function of an HVDC system can be obtained by the analytical solutions. The insights for the six pulse system can easily be adopted to

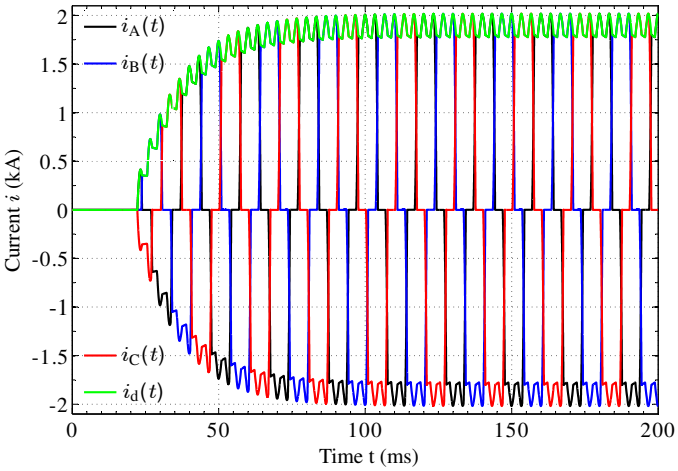

Fig. 10: Currents of the rectifier over the entire simulation period with the analytical model implemented in MATLAB®

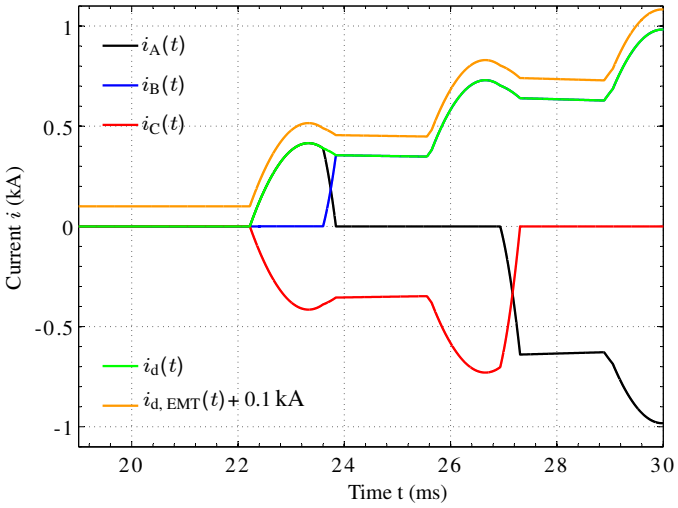

Fig. 11: Currents of the rectifier in the start-up period with the analytical model compared with i_d of the EMT model implemented in SIMULINK®

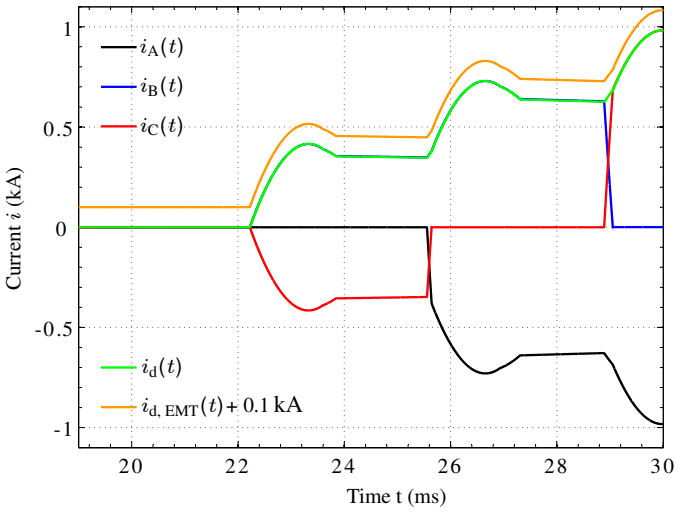

Fig. 12: Currents of the inverter in the start-up period with the analytical model compared with i_d of the EMT model

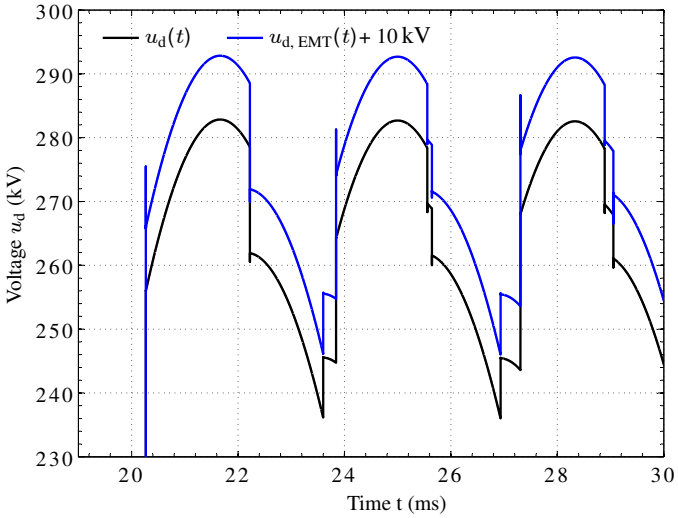

Fig. 13: Output voltage of the rectifier in the start-up period of the analytical model compared with the EMT model

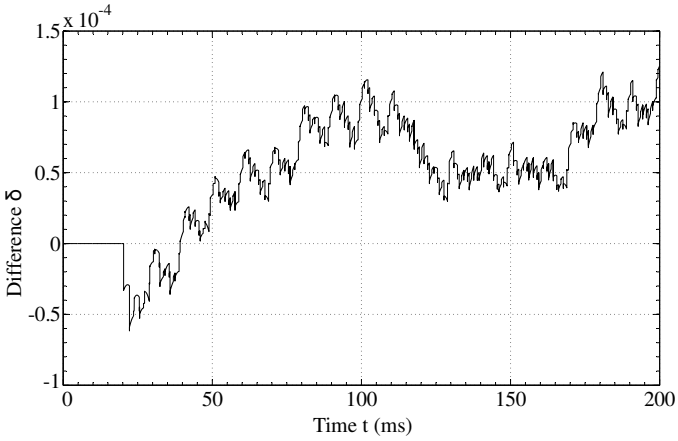

Fig. 14: Difference between DC current i_d of the analytical model and the EMT model for simulation of complete HVDC system

different configuration, e.g. a twelve pulse HVDC converter can be regarded as two six pulse converters in series for which analytical solutions have been derived in this paper.

Acknowledgment

The authors gratefully acknowledge the contribution of Diren Toprak in his thesis at the Chair of Electrical Energy Systems in 2013.

References

[1] J. Dorn, H. Gambach, and D. Retzmann, "HVDC transmission technology for sustainable power supply," in *9th International Multi-Conf. on Systems, Signals and Devices (SSD)*, Chemnitz, March 2012, pp. 1–6.

[2] G. Kamalapur, V. Sheelavant, S. Hyderabad, A. Pujar, S. Baksi, and A. Patil, "HVdc transmission in India," *Potentials, IEEE*, vol. 33, no. 1, pp. 22–27, Jan 2014.

[3] L. Cheng, H. Feng, and J. He, "HVDC development and its reliability in China," in *Power and Energy Society General Meeting (PES), 2013 IEEE*, July 2013, pp. 1–5.

[4] B. Schucht, K. Kleinekorte, M. Fuchs, and R. Joswig, "German grid development plan 2013 - second draft of the transmission system operators (German title: Netzentwicklungsplan Strom 2013 - Zweiter Entwurf der Übertragungsnetzbetreiber)," http://www.netzentwicklungsplan.de/NEP_2013_2_Entwurf_Teil_1_Kap_1_bis_9.pdf, 2013 (accessed March 10, 2014).

[5] R. Kumar and T. Leibfried, "Analytical Modelling of HVDC Transmission System Converter using Matlab/Simulink," in *Industrial and Commercial Power Systems Technical Conference, 2005 IEEE*, Saratoga Springs, NY, May 2005, pp. 140–146.

[6] G. Herold, *Electrical power supply V (German title: Elektrische Energieversorgung V)*. Schlembach Fachverlag, 2009, ISBN: 978-3-935340-65-6.

[7] C. Hahn, A. Müller, and M. Luther, "A novel approach to select HVDC - controller parameters by using a decoupling filter," in *International Conference on Renewable Energies and Power Quality (ICREPQ'13)*, Bilbao, 2013.

Biographies

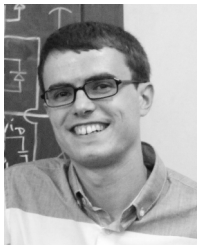

Leonhard Probst was born in 1991. He received his B.Sc. degree from University of Erlangen-Nuremberg, Germany, in 2014. Currently he is an exchange student with Power Electronics Group at Indian Institute of Science, Bangalore. His research interest is control and simulation of high power converters.

Christoph Hahn received his Dipl.-Ing. degree from the University of Erlangen-Nuremberg, Germany, in 2011. Currently he is a Ph.D. student and research associate at the Chair of Electrical Energy Systems at the University of Erlangen-Nuremberg, Germany. His research interests lie in the field of HVDC modeling and control.

Matthias Luther studied electrical engineering and received his Ph.D. at the Technical University of Brunswig, Germany in 1992. From 1993 he held different functions and management positions in the electricity industry at PreussenElektra, E.ON Netz and TenneT TSO. Since 2011 he is professor and holds the Chair of Electrical Energy Systems at the University of Erlangen-Nuremberg, Germany.